THE JOURNAL OF PHYSICAL CHEMISTRY B

Article

pubs.acs.org/JPCB

Polymer Translocation through a Nanopore: DPD Study

Kan Yang,[†,‡] Aleksey Vishnyakov,[†] and Alexander V. Neimark*,[†]

[†]Chemical and Biochemical Engineering, Rutgers University, 98 Brett Road, Piscataway, New Jersey 08854, United States

[‡]State Key Lab for Mineral Deposit Research, School of Earth Sciences and Engineering, Nanjing University, 22 Hankou Road, Nanjing, 210093 P. R. China

Supporting Information

ABSTRACT: Translocation of a polymer chain through a narrow pore is explored using 3D explicit solvent dissipative particle dynamics simulation. We study the dependence of the translocation dynamics and translocation time τ on the chain length N, driving force magnitude E, and solvent quality. Two types of driving forces are considered: uniform hydrostatic force, which is applied equally to the chain and solvent particles, and uniform electrostatic force, which is applied selectively to the charged particles in the chain and oppositely charged counterions in the solvent. We concluded that the scaling correlations $\tau \sim E^{-\xi}$ and $\tau \sim N^{\beta}$ are valid only for coil-like chains. For globular chains, the exponents ξ and β could not be identified with a reasonable accuracy. While the found value of ξ agrees with published experimental results and does not depend on the driving force type, the exponent β depends on the driving force and solvent quality. This is explained by nonequilibrium effects, as in the systems considered, the time of translocation is comparable with the time of chain relaxation. These effects, manifested in the changes of chain conformation in the process of translocation, were analyzed on the basis of the variation of the gyration radii of *cis* and *trans* segments of the chain in normal and lateral directions. A prominent chain expansion was observed for coils and was insignificant for globules. This work demonstrates the feasibility of the 3D dissipative particle dynamics modeling of translocation phenomena and accounting for the electrostatic interactions with explicit counterions, as well as for the solvent quality, in a computationally efficient manner.

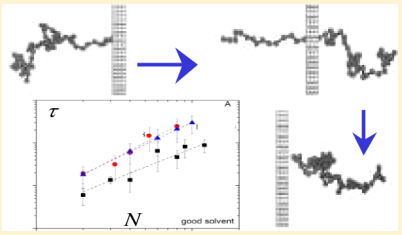

1. INTRODUCTION

Translocation of polymers through nanoscale pores is a complex physical process of great importance for various biological phenomena such as injection of viral DNA, RNA transfer across nuclear pores, and protein transport through membrane nanopores,[1,2] as well as for chromatographic separation and purification of natural and synthetic polymers and biomolecules on nanoporous substrates.[3]

In order to thread through an opening that is much smaller than its radius of gyration, a polymer chain has to assume an elongated conformation that is entropically unfavorable. This entropy toll on the chain free energy creates a barrier, which can be overcome by an external driving force. Polymer translocation has attracted a great deal of attention in the literature. Experimental studies typically deal with penetration of polymer coils dissolved in a good solvent through nanopores of biological or solid state membranes driven by a constant electrostatic force. In their pioneering paper, Kasianowicz et al.[4] reported experimental investigations of translocation of single-stranded RNA and DNA molecules through a lipid bilayer with α-hemolysin pores of ~2.6 nm in diameter. The translocation event was detected as a prominent drop of the ionic current due to a partial pore blockage by the moving chain. The duration of the current drop was associated with the translocation time. The authors distinguished "short-time" and "long-time" blockages, which may be related, in fact, to failed and successful translocation attempts. In later experiments,[5−7] similar setups were employed with various single- and double-stranded DNA translocating through nanopores in biological and solid state membranes. The relationships between the translocation time τ and the key system parameters, such as the chain length N and driving force magnitude E, are traditionally interpreted in terms of scaling correlations, such as $\tau \sim N^{\beta}$ and $\tau \sim E^{-\xi}$, with the scaling exponents ξ and β that are commonly assumed to be independent of each other. Experimental data for globular proteins, for which water is a poor solvent, is limited.[5−7] In the process of translocation, the globule should open up as suggested by Talaga and Li,[5] who explored translocation of β-lactoglobulin through a pore in a silicon nitride membrane (see also a comprehensive review in ref 8).

A number of simulations and theoretical calculations have been performed using various models of polymer chain dynamics. It is worth noting that atomistic level simulations, in particular molecular dynamics (MD), which are very impressive and demonstrative, are still prohibitively expensive, e.g., ref 9. Indeed, even with specially designed high performance algorithms, it takes 24 h for thousands of CPUs to compute one all-atom trajectory of translocation of just 10 nucleotides through a nanopore.[9] Taking into account that we deal here with a stochastic process, it is necessary to perform multiple runs to collect statistically meaningful data. This

Received: October 22, 2012
Revised: February 27, 2013
Published: March 6, 2013

challenge can be met by a coarse-grained representation of biomolecules. Most authors used an ideal Gaussian chain model[10−12] or a bead−spring model with short-range repulsion between the beads.[13−15] The computational methods include various one-dimension diffusion models,[10−12,16,17] solvent-free kinetic Monte Carlo (MC),[13,18−22] coarse-grained molecular dynamics (CGMD),[15,23−26] Brownian/Langevin dynamics (BD/LD),[27] and dissipative particle dynamics (DPD).[15,28,29] The resulting scaling exponents vary substantially depending on the method, dimensionality of the system, and the type of the driving force applied (there are also a few studies of purely diffusive translocation unassisted by a driving force[30]). In modeling studies, the driving force was applied either explicitly as a local force acting on the beads located within the pore[13,17,31] or implicitly by setting a difference in polymer chemical potential in the *cis* and *trans* compartments. This difference is created by distinct polymer−solvent[15,16,30] or polymer−solid[11,20] interactions on *cis* and *trans* sides of the membrane. In these cases, the driving force is essentially independent of the chain length, and thus, the scaling exponents β and ξ should be independent as well. Alternatively, the driving force can be applied to all or selected beads of the chain, or uniformly to all beads, including solvent if the latter is modeled explicitly[32] and, as such, be proportional to *N*. Recently, He et al.[32] in 2D DPD simulations and Kapahnke et al.[15] in 3D DPD simulations reported that there exists a significant dependence of the scaling exponent β on the magnitude of the driving force, casting doubts on an adequacy of the universal scaling exponent description of translocation phenomena.

In this work, we model the translocation of chain molecules in coil and globule states through nanopores using 3D DPD simulations. The DPD method allows us to consider the polymer−solvent interactions explicitly, which is especially important in studies of charged polymers driven by electric forces, when the dissociated counterions should be taken into account. Most importantly, the DPD method, which operates with soft quasi-particles, provides a significant improvement of computational efficiency compared to the MD and other methods that employ hard-core interaction potentials of Lennard-Jones type (e.g., recent ref 33). Also, the size of the bead of the coarse-grained polymer chain can be chosen commensurate with the pore opening, thus ensuring that the pore cross section can accommodate only one bead. This natural coarse-graining helps simplify the simulation setup and enables comparison with the earlier simulations, where the condition of one bead in the pore cross section was implied. It is worth noting that the DPD method was shown efficient in modeling polymer translocation; however, all but two previously published works were limited to 2D models.[32] The 2010 work of Kapahnke et al.[15] was the first attempt of 3D DPD simulation of translocation phenomenon. The authors studied the chain translocation driven by a contrast in the solvent quality on the *cis* and *trans* sides of the membrane that is equivalent to the application of the local force inside the pore. Several very recent papers employed the hard-core interaction potentials with the 3D DPD simulation scheme to avoid particle overlap.[25,28,29] In particular, Li et al.[28] explored polymer translocation driven by electrostatic field through relatively wide channels and obtained the scaling exponents β and ξ for different solvent quality and driving force magnitude. The same group studied the dependence of translocation dynamics on the length of the channel between *cis* and *trans* compartments.[29] Feng et al.[25] reported different scaling exponents depending on the choice of the range of dissipative interactions. Another just published paper[26] employs LJ hard-core potentials with the Langevin thermostat; this paper considers different features of the translocation process, such as the translocation time dependence on channel length. Noteworthy, the use of soft potentials is the most attractive feature of the DPD method that makes it computationally efficient compared to the MD and MC models with hard-core interactions between beads.

The methodological novelty of this work is in the demonstration of the feasibility of the 3D DPD method for modeling the translocation phenomena and accounting for the electrostatic interactions with explicit counterions, as well as for the solvent quality, in a computationally efficient manner (compared with hard-potential models). We performed 3D DPD simulations with two different types of driving forces: (i) a spatially uniform hydrostatic-type force, which equally acts on polymer and solvent beads, and (ii) a spatially uniform electrostatic-type force, which acts only on the charged beads within the polymer chain and on the counterions in solution. In the latter case, we consider explicitly, for the first time in the translocation literature, the electrostatic interactions between charged fragments of the polymer and counterions in the solution. In doing so, the charges are either equally distributed between the beads of the chain, as is done in modeling uniform polyelectrolytes such as sulfonated polystyrene or DNA (this model will be referred to as "uniform chain model") or assigned to the selected beads to mimic a heterogeneous charge distribution in proteins (this model will be referred to as the "heterogeneous chain model"). These models were chosen for their simplicity and qualitative difference; in the uniform chain model, the force is proportional to the chain length, while in the heterogeneous chain model, the force is independent of the length. We analyze the dependence of the translocation time on the chain length, the driving force magnitude, and the solvent quality. Special attention is paid to the alteration of chain conformations in the process of translocation in good and bad solvent, which has only been briefly discussed in the literature.[32] An analysis of polymer conformation is especially important for studies of translocation of globular proteins.

The rest of the paper is structured as follows. In section 2, we briefly present the DPD methodology employed to simulate the translocation process and describe the interaction parameters, as well as the simulation system setup. In section 3, we demonstrate that the adopted simulation model provides a proper description of the coil−globule transition, and thus is suitable for studies of the effects of solvent quality. In section 4, we study the effect of the driving force magnitude for the case of good solvent. In section 5, we present results of the influence of the solvent quality, which was varied from good to bad conditions, on the translocation time for different driving forces. In section 6, we consider chain conformations during the translocation process. The conclusions are summarized in section 7.

2. SIMULATION SETUP AND TECHNIQUES

We used a standard version of the DPD technique,[34] as summarized in ref 35. The polymeric molecule is presented by a chain of quasi-particles, or beads of equal diameter R_c. The interactions between beads *i* and *j* include soft conservative repulsion force, random force, and velocity dependent friction drag force: $\mathbf{F}_{ij} = \mathbf{F}_{ij}^{(C)} + \mathbf{F}_{ij}^{(R)} + \mathbf{F}_{ij}^{(D)}$. We applied a standard form

dx.doi.org/10.1021/jp3104672 | J. Phys. Chem. B 2013, 117, 3648−3658

of the conservative force, which decays linearly with the distance between the beads r_{ij}, with the cutoff potential radius of action equal to R_c: $\mathbf{F}_{ij}^{(C)} = a_{ij}(1 - r_{ij}/R_c)(\mathbf{r}_{ij}/r_{ij})$, if $r < R_c$; and $\mathbf{F}_{ij}^{(C)} = 0$, if $r \geq R_c$. As such, R_c is treated as the bead diameter, which is assumed equal for all quasi-particles in the system. Here, a_{IJ} is the conservative parameter specific to the bead types I and J to which particles i and j belong, and $\mathbf{r}_{ij}$ is the vector between the ith and jth particles. The repulsion force acts along the line connecting the centers of the beads. The repulsive parameter for solvent beads is set to $a_{ss} = 25kT/R_c$, and the system density is set to $\rho R_c^3 = 3$, as recommended for aqueous solutions.[36] The random force, which accounts for thermal fluctuations, is taken proportional to the conservative force that is also acting along the vector between the bead centers: $\mathbf{F}_{ij}^{(R)}(r_{ij}) = \sigma w^R(r_{ij})\theta_{ij}(t)\mathbf{r}_{ij}$, where $\theta_{ij}(t)$ is a randomly fluctuating in time variable with Gaussian statistics. The drag force is velocity-dependent: $\mathbf{F}_{ij}^{(D)}(\mathbf{r}_{ij}, \mathbf{v}_{ij}) = -\gamma w^D(r_{ij})(\mathbf{r}_{ij}*\mathbf{v}_{ij})$, where $\mathbf{v}_{ij} = \mathbf{v}_j - \mathbf{v}_i$ and $\mathbf{v}_i$ and $\mathbf{v}_j$ are the current velocities of the particles. We assume the common relationship between the drag and random force parameters $w^D(r) = [w^R(r)]^2$ and $\sigma^2 = 2\gamma kT$ ($\sigma = 4.5$). Noteworthy, the pairwise random and friction force employed in DPD secure the conservation of momentum, which is not conserved in BD or MD models with the original Langevin thermostat based on single particle random and friction forces. This is the main methodological advantage of DPD for the conservation of momentum is critically important in studies of hydrodynamic problems like translocation.

For charged beads in the simulations with the electrostatic driving forces, we applied the "smeared charge" model of Groot[37] recently employed in simulations of dendrimer–lipid interactions.[38] The charge is distributed as a symmetric cloud of linearly decreasing density centered at the center of bead i, $\rho_i(|\mathbf{r} - \mathbf{r}_i|)/e_i = f(|\mathbf{r} - \mathbf{r}_i|) = 3(1 - (|\mathbf{r} - \mathbf{r}_i|/R_e)/\pi R_e^3$, where e_i is the total bead charge and R_e is the smearing radius set to $R_e = 1.6R_c$, similarly to ref 37, were static properties of similar polyelectrolyte were studied. As such, the electrostatic potential between two charged beads i and j screened by the medium with dielectric constant ε_r is given by a nondiverging integral $V_{ij}^e = \int\int f(|\mathbf{r}_1 - \mathbf{r}_i|)\Gamma/(4\pi|\mathbf{r}_1 - \mathbf{r}_2|)f(|\mathbf{r}_2 - \mathbf{r}_i|)d^3\mathbf{r}_1\, d^3\mathbf{r}_2$, where Γ is the coupling constant $\Gamma = e_i e_j/kT\varepsilon_0\varepsilon_r R_c$.[37] The connectivity of the chain beads is ensured by a spring force acting between neighboring beads: $F_B = -K_B(r_{ij} - r_{eq})\mathbf{r}_{ij}/r_{ij}$, where $K_B = 100\ kT/R_c$ is the spring elastic constant and $r_{eq} = 0.8R_c$ is the equilibrium bond length. We set $\varepsilon_r = 78$, as in pure water at ambient temperature.

With the uniform electrostatic force, we attempted two different types of charge distribution along the chain: (i) the total charge is fixed, and the driving force is independent of N. This manner of applying the driving force, which we will call the heterogeneous chain model, crudely mimics the translocation of proteins, which can be differently coarse-grained. To consider a particular example, we "mapped" the charge profile of β-lactoglobulin (βLGa) at neutral pH onto the model chain of coarse-grained beads. The charge profile of βLGa is presented in the Supporting Information, Figure S1. Depending on the level of coarse-graining, each bead contained a certain number of amino acids. The charges of the amino acids within each bead were summed up, and this sum was assumed as the bead charge. The sum of bead charges along the chain equaled the total charge of βLGa −10e. To satisfy the electroneutrality, charged counterions (positive and negative) modeled as charged solvent beads were added to the solvent. The heterogeneous charge distribution has some major consequences. First, the charge profile of βLGa (like many other proteins) is inhomogeneous. Most of the negative charges are concentrated in the tail of the chain (that is, the beads that are the last to enter the opening), while the head section, which enters the opening first, is slightly positively charged and therefore experiences force opposite to the translocation direction. The central section of the polymer also bears a positive charge. Second, the interactions between explicit charges of the chain, as well as with the hydrophilic counterions, affect the conformations of the translocating protein, especially in bad solvent, effectively making it more hydrophilic. Since the polymer charge remained constant and the chain length varied, polymer beads were allowed integer charges stronger than $\pm e$, but all counterions were assigned $+e$ or $-e$ charge, and each charged bead was neutralized by one or more counterions. Accordingly, the number of counterions changed from 10 (all positive) at $N = 1$ (single bead) to a maximum of 29. Assuming that each solvent bead effectively models three water molecules, the concentration of counterions varies approximately from 0.02 to 0.08 M, which is sufficient to affect substantially the conformations of the translocating chain as well as the translocation time.

(ii) In the second model, each bead carried a fixed amount of charge, which is independent of the chain length. In this case, the total charge and, correspondingly, the driving force acting on the chain are proportional to the chain length N. This model is referred to below as the "uniform chain model". In the uniform model, electrostatic repulsion interactions between the polymer beads and counterions were omitted, which meant they do not affect conformations of the translocating polymer. The uniform chain model is therefore similar to one under the hydrostatic driving field, but the driving force is only applied to the polymer beads rather than to all beads. The absence of intrachain electrostatic interactions and the uniformity of the driving field make our setup different from that in current blockage experiments[4,5,39] where the driving force depends strongly on the bead location.

The simulation cell had a cylindrical shape with periodic boundary conditions applied in the axial x-direction (Figure 1). The sizes of the cell were $30R_c$ in length and $20R_c$ in diameter. The cell walls were composed of implicit immobile DPD beads "smeared out" over the outer space outside the cylindrical

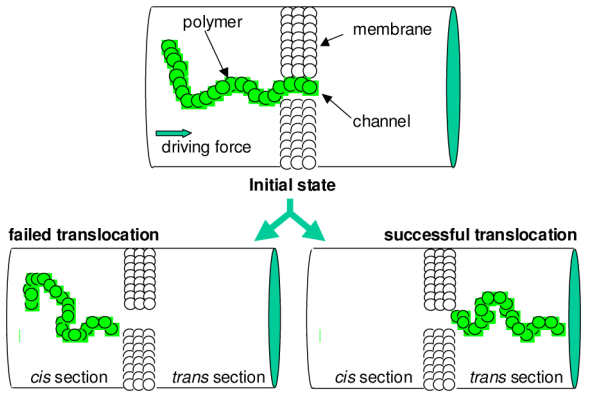

Figure 1. Simulation setup. In the initial configuration, the polymer is placed in the *cis* compartment (shown on the left side of the membrane) with the first three beads located within the pore. The chain is relaxed with the driving force turned off and the second bead fixed at the pore center. At time zero, the driving force is applied.

dx.doi.org/10.1021/jp3104672 | J. Phys. Chem. B 2013, 117, 3648−3658

system. The density of implicit beads was equal to the average density in the system $\rho R_c^3 = 3$, which was repulsive to both polymer and solvent with the parameters of $a_{WP} = a_{WS} = 55kT/R_c$ (here and further on, subscript index "P" refers to the polymer, "S" to solvent, "W" to the wall, and "M" to the membrane). The cylindrical cell was separated into *cis* and *trans* compartments by a membrane that consisted of three layers of repulsive beads (4314 beads in total). By using three layers of repulsive beads, we make sure that the probability of penetration of solvent and polymer beads through the membrane is negligible. The membrane had a pore of circular cross-section of $2.2R_c$ in diameter (counted as the distance between the centers of immobile beads that form the membrane), as shown in Figure 1. The positions of the membrane beads were fixed throughout the simulation.

In the initial configuration of each simulation, the polymer molecule was placed in the *cis* compartment with the three end beads already in the channel (Figure 1). The chain was relaxed with the driving force turned off. Coordinates of the second bead were fixed at the center of the pore throughout the relaxation process. No restrictions were applied to other mobile beads such as solvent and counterions. The counterions were dissociated with practically no ion pairs observed. They tended to spread throughout the system. At time zero, the driving force was applied, the chain was released, and the translocation process began. If the entire chain exited the opening to the *trans* compartment, the translocation was considered successful. The time at which the last chain bead crossed the plane formed by the centers of the rightmost layer of membrane beads was recorded as the translocation time τ. If the entire chain exited the channel to the *cis* compartment, the translocation is counted as "failed" and the simulation stopped. The duration of the fail translocation event was recorded as well.

3. CONDITIONS OF THE COIL–GLOBULE TRANSITION

To show that the model chosen is capable of describing polymer behavior in good and bad solvent, we determined the conditions of the coil–globule transition. For this purpose, we simulated free uncharged polymer chains in a large solvent bath under 3D periodic boundary conditions with solvent–solvent and polymer–polymer repulsive parameters $a_{SS} = a_{PP} = 25kT/R_c$ and polymer–solvent repulsive parameter a_{PS} being varied. The state of the polymer chain was detected using the correlation between the chain length and the radius of gyration in the form of the power law $R_g \sim N^{\nu}$ and is quantified with the Flory exponent ν. The results are presented in Figure 2. When the solvent is poor (that is, a_{PS} is high), the chain collapses into a globule with the volume proportional to the chain length ($\nu \approx 1/3$). As the solvent–polymer interactions become less repulsive, the polymer exhibits a continuous transition to a random coil signified by the increasing ν. We could see that θ-solvent conditions ($\nu = 1/2$) correspond in the DPD model to $a_{PS} = 27.25\ kT/R_c$; see Figure 2. This result agrees within the accuracy of these calculations with data reported recently.[15] Using a widely adopted linear correlation between the interaction contrast $\Delta a = a_{PS} - a_{SS}$ and the Flory–Huggins parameter, $\chi = 0.286\Delta a$,[35] we estimate the θ point value of $\chi_\theta = 0.63$. As the solvent–polymer interactions improve further, ν stabilizes in the 0.56–0.64 interval, which includes the values obtained previously for self-avoiding polymer chains using different methods, including similar 3D DPD simulations.[40−42] In further simulations of translocation, most of the simulations were performed with $a_{PS} = 25kT/R_c$ ($\chi = 0$, good solvent, unconstrained polymer chain adopts a coil configuration) and $a_{PS} = 40\ kT/R_c$ ($\chi = 4.29$, bad solvent, polymer chain assumes a globular state).

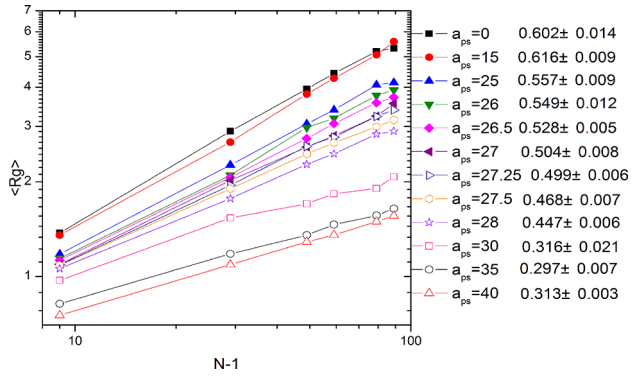

Figure 2. DPD simulation of the coil–globule transition. Correlations between the chain length and the radius of gyration of a single chain at different solvent qualities characterized by the polymer–solvent interaction parameter a_{PS}. The error bars for the scaling exponent given in this figure are calculated under the assumption that the scaling exponent is a normally distributed random variable and correspond to 90% percentile. The linear regressions are calculated using the least-squares algorithm.

4. DRIVING FORCE EFFECT IN GOOD SOLVENT

The scaling between the translocation time τ and the driving force magnitude E was extensively studied in the literature both experimentally and with simulations for coil-like chains at the good solvent conditions. Assuming the standard power law scaling, $\tau \sim E^{-\xi}$, Kasianowicz et al.[4] obtained an inverse proportional dependence with the scaling exponent $\xi = 1$. This intuitively plausible result, the stronger the force the shorter the time, was confirmed by later studies of single-stranded and double-stranded DNA translocation through solid and α-hemolysin pores.[5,43,44] Meller et al.[39] found strongly nonlinear dependence of the polymer velocity on the applied voltage. On the theoretical front, numerous kinetic MC and LD/BD simulations in 2D and 3D with the "local" driving force confirmed the inverse proportional correlation $\xi \approx 1$.[19,27,45−48] Ikonen et al.[49] in their MD and theoretical study of polymer translocation found a nonuniform correlation between τ and E, with $\xi \approx 0.9$ for weaker driving forces and $\xi \approx 1$ for stronger forces. They concluded that translocation time could not be described with a universal set of scaling exponents and stressed the importance of pore–polymer interactions that contributed substantially to the nonuniversal polymer behavior. There is also a significant dissent. He et al.[32] modeled polymer translocation by 2D DPD with a uniform hydrostatic force applied to all beads, polymer, and solvent, and obtained $\xi \approx 1/2$. Kantor and Kardar[16] in their 2D MC simulations obtained the scaling exponents of $\beta = 1.875$ and $\xi = 1.45$ when the polymer was pulled from one end and driven by a chemical potential difference, correspondingly. $\xi = 2.0$ correlation was observed in 2D dynamic MC simulations of Chen et al.,[50] and 3D explicit solvent MD simulations of Matysiak et al.[23] Later, Luo et al.[51,52] reported a complex picture with several intervals of the driving force characterized by different values of ξ, including $\xi = 1$ at sufficiently strong forces.

For examination of the driving force influence on τ, we consider polymer chains of 80 beads driven by uniform hydrostatic and electrostatic driving forces at the good solvent

dx.doi.org/10.1021/jp3104672 | J. Phys. Chem. B 2013, 117, 3648−3658

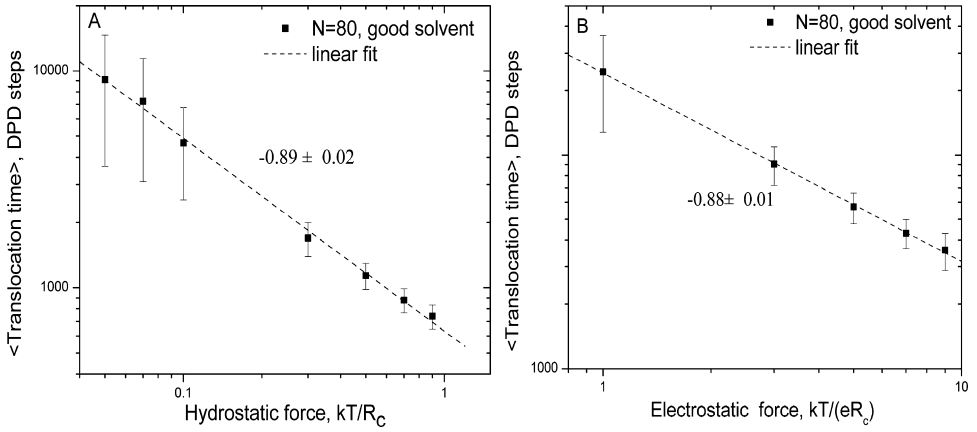

Figure 3. Translocation time dependence on the driving force magnitude for $N = 80$ in good solvent: (a) uniform hydrostatic driving force; (b) uniform electrostatic driving force, heterogeneous chain model. Each point shown is the average of at least 1000 successful translocation events. The slopes of the linear fit are -0.89 ± 0.02 (a) and -0.88 ± 0.01 (b), correspondingly. Uncertainties are given at 90% confidence level.

conditions. The range of driving field magnitude for each force type was chosen so that the driving force acting on one bead in a polymer chain was substantially weaker compared to the mean conservative repulsion force acting between the soft beads in DPD simulation but strong enough so that reliable statistics could be obtained. The magnitude of the driving force acting on a bead varied from 0.05 kT/R_c to 0.9 kT/R_c for hydrostatic force and from 1.0 kT/R_c to 9.0 kT/R_c for electrostatic force. This means that the strongest driving forces were comparable to the typical repulsive forces between the individual beads in our DPD system, while the weakest driving forces were much weaker than the interparticle forces. Generally, when the electrostatic force is applied, the beads move through the resisting viscous solvent. The oppositely charged counterions add to this resistance. Contrary to that, the hydrostatic force affects all beads, and as such, both the chain and the solvent form a flow driven through the pore. Note that the hydrostatic force employed here does not correspond to the pressure driven flow considered in MD studies of water ultrafiltration through nanopore.[53,54]

Despite the different nature of the flow, the correlation between the force magnitude E and τ is very similar for both driving force types (Figure 3). Here and further on, each point shown is obtained as an average of at least 1000 successful translocations. The weaker the driving force, the longer is the translocation time, and the more expensive the simulations are. That is why the statistical error is greater for weaker forces. The ranges of magnitudes of driving forces acting on the entire chain were approximately the same for all field types: 0.4–80kT/R_c for the hydrostatic field and 0.6–90 kT/R_c for the electrostatic filed. However, the translocation times obtained with the electrostatic field were substantially slower. In both cases, there is a reliable linear correlation between the logarithms of the translocation time τ and the force magnitude E with the slope of $\xi \approx 0.9$. This result is close but not equal to the trivial inverse proportional scaling, $\xi = 1$, observed in experiments and simulations reported previously,[4,19,23,46,52] and rather coincides with the MD result obtained in ref 49 for weaker driving force and a recent DPD simulation.[26] This finding is likely to indicate the importance of an explicit solvent model when translocation phenomena are considered.

5. CHAIN LENGTH DEPENDENCE. INFLUENCE OF THE SOLVENT QUALITY

A linear increase of the translocation time with the chain length ($\tau \sim N^{\beta}$, $\beta = 1$) was reported for single-stranded DNA by Kasianowicz et al.[4] and later by Meller et al.[39] Storm et al.[44] experimented with much stiffer double-stranded DNA and solid silicon oxide pore, and reported a higher scaling exponent, $\beta = 1.27$, that was also obtained in a number of theoretical and simulation studies, which employed 2D DPD,[32] MD,[23] BD/LD,[25,27,30,31,52] 2D and 3D dynamic MC,[13,19,45,50] and a complex 3D multiscale methodology combining constrained MD for the polymer motion with a lattice-Boltzmann treatment of the solvent hydrodynamics.[24] However, in other works, higher values of β, ranging up to 2.5, were obtained.[15,18,20−22,46,48,51,52,55−57] Some authors found different scaling exponents for different chain lengths[48] and driving force magnitudes. There were also several attempts to establish correlations between scaling exponent β and Flory exponent ν for translocation in 2 and 3 dimensions. For example, Sung and Park[10] studied translocation of ideal chains by using self-consistent field theory (SCFT) and obtained $\beta = 2 + \nu$ at very weak driving forces; as the driving force became stronger, the translocation time encountered a crossover in the scaling behavior from $\beta = 2 + \nu$ at very weak driving force to $\beta = 1 + \nu$ at stronger driving forces. The same correlation, $\beta = 1 + \nu$, was suggested by Dubbeldam et al.[21] and Tsuchiya and Matsuyama.[18] Later, Park and Sung[11] studied the temperature dependence of translocation driven by polymer adsorption on the *trans* side of the membrane. They found that the correlation between τ and N differed above and below T_c, the temperature of adsorption−desorption transition, for ideal polymer chains on the *trans* side: $\beta = 2$ at $T > T_c$ and $\beta = 3$ at $T < T_c$. Using SCFT calculations, Muthukumar[58] studied translocation of polymer chains with excluded volume interactions and obtained $\tau \sim N$. Matysiak et al.,[23] Wei et al.,[30] and Bhattacharya et al.[52] reported $\beta = 2\nu$, while the relationship $\beta = 1 + 2\nu$ was reported by Milchev et al.,[20] Romiszowski and Sikorski,[22] and Lehtola et al.[46] Very recently, Qian et al.[59] obtained $\beta = 2.35$ for a partially charged polymer under uniform electrostatic driving field. And last, Feng et al.[25] obtained in 3D DPD simulation with LJ interactions between the particles the scaling exponents $\beta \sim 1$ that are significantly smaller than all other reported values. In addition, disagreement between the value of β determined with

dx.doi.org/10.1021/jp3104672 | J. Phys. Chem. B 2013, 117, 3648−3658

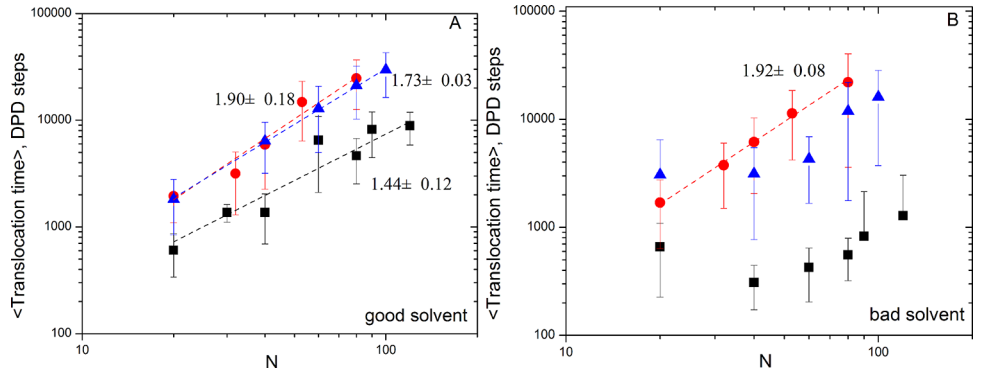

Figure 4. Dependence of the translocation time τ on the chain length N at good (A) and bad (B) solvent conditions. Different symbols correspond to different models considered: squares, uniform hydrostatic force; circles, uniform electrostatic force, heterogeneous chain model; triangles, uniform electrostatic force, uniform chain model. Slopes for the linear fit performed for $N \geq 20$ are shown on the charts by broken lines with the respective estimates of the scaling exponents β. The linear correlations are based on τ obtained in 1000 individual successful translocation events, rather than on the average translocation times shown by symbols on the plots. The "uncertainties" demonstrated by thin vertical lines show an interval within which 90% of observed τ values fall at given N. Note that the linear regressions are shown for the conditions at which the chain remained coil-like in the course of translocation. The scaling relationship for globular chains could not be identified with reasonable accuracy.

the explicit-solvent[28,49] and implicit-solvent models shows the importance of accounting for explicit solvent in simulations of polymer dynamics.

We explored the dependence of the translocation time τ on the chain length N under the uniform hydrostatic and electrostatic driving forces in good and bad solvents. The results for chains ranging from $N = 20$ to $N = 120$ are presented in Figure 4 in double logarithmic coordinates. The power law correlation between τ and N seems applicable to the systems considered under good solvent conditions (Figure 4a), for which β was determined with a reasonable accuracy at $N > 20$. For the uniform hydrostatic force, the scaling exponents were determined as $\beta \approx 1.44$, which is generally consistent with the $\beta = 1 + \nu$ correlation based on the chi-square criterion, in contrast to other possible correlations ($\beta = 1$, $\beta = 2\nu$, $\beta = 1 + 2\nu$, $\beta = 2$). With electrostatic driving force, both uniform and heterogeneous models produced a higher scaling exponent that is inconsistent with the previously reported values of β. The steepest increase of τ with N is observed for the heterogeneous model, which is natural because the overall driving force in this case is constant and does not depend on the chain length.

Under bad solvent conditions (Figure 4b), a reasonable scaling was found only for the heterogeneous model. In this case, the value of β obtained was nearly identical to that in good solvent. This unexpected result can be explained by the fact that the chain due to the strong electrostatic charges did not comprise into a globule but generally assumed open configurations. This is confirmed by the analysis of configurations of *cis* and *trans* subchains discussed below (section 6). The difference in the translocation process for coils and globules is illustrated in Figure 5, where we present a series of snapshots taken at the different degrees of translocation (0, 25, 50, 75, and 100%) in real simulation time. Typical snapshots of a chain simulated with the heterogeneous chain model are shown in Figure 5b. Despite the fact that apparent local compaction of fragments of the chain is observed, the chain generally maintains a stretched, coil-like configuration.

In the uniform chain model, where the electrostatic forces between the beads are weak and do not affect the polymer conformation, the chain under bad solvent conditions remained in a well-defined globular conformation (Figure 5a) throughout the translocation process, in *cis* and *trans* compartments alike, similarly to the chain under hydrostatic field. The translocation mechanisms for coil and globular polymers are inevitably different, especially at large N. Indeed, both the work needed to transfer the center of mass of the tethered chain from the *cis* to *trans* compartment and the friction coefficient are proportional to the chain effective diameter, which is smaller for the globule and scales as $N^{1/3}$ for globules and $N^{0.6}$ for coils. As such, the time for the globule translocation should be smaller than the time for the coil translocation at the same driving force, as seen from Figure 4. We also should expect a smaller β exponent for globules compared to that for coils. This is confirmed qualitatively by the data in Figure 4, especially for the hydrostatic force, when the chain transformation is not affected by electrostatic repulsion and the difference between the coil in good solvent and the globule in bad solvent is well pronounced. However, the time−length relationship for globular chains does not show a power law scaling with reasonable accuracy, at least for the chain lengths considered here. One of the possible explanations is that translocation of globules occurs much faster than translocation of coils and the statistics was insufficient even though the data was collected over 1000 successful translocation events.

From the comparison of the scaling exponents for translocations in good and bad solvents for the hydrostatic force, we concluded above that translocation time increases with chain length faster under good solvent conditions. This conclusion is supported by the simulations, in which the solvent−polymer/solvent−solvent interaction contrast a_{PS} was varied. For example, Figure 6a shows the correlation between τ and a_{PS} for $N = 30$. It is obvious that the better the solvent, the larger the translocation time is. A similar result was obtained by He et al.[32] in 2D DPD simulation with the hydrostatic driving force. The translocation time decreases roughly linearly with a_{PS}, and respectively, it increases linearly with the Flory−Huggins parameter χ. However, given the different scaling exponents β in $\tau(N)$ dependences for coil and globule polymers, one cannot expect a universal scaling relationship between the translocation time and the solvent quality. In particular, Figure 6b shows that the solvent quality has a greater influence on longer chains compared to shorter chains.

The influence of the driving force magnitude on β may be explained by a nonequilibrium nature of the process: if the

dx.doi.org/10.1021/jp3104672 | J. Phys. Chem. B 2013, 117, 3648−3658

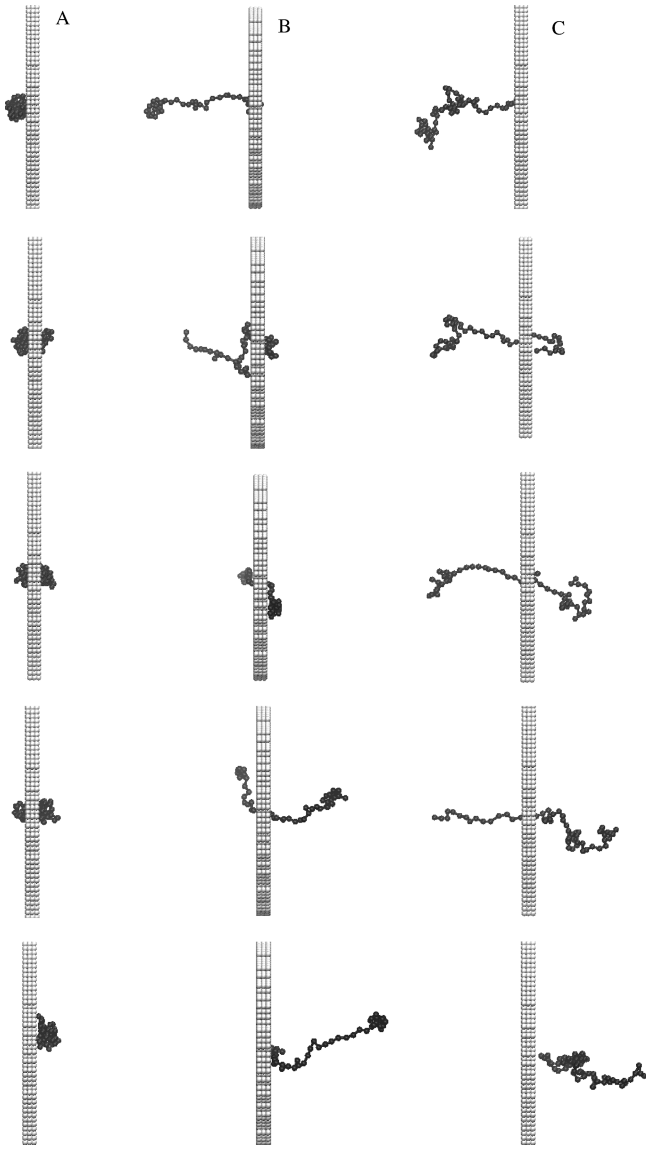

Figure 5. Sample snapshots of the translocating chain at different solvent conditions and degrees of translocation. Column A, uniform chain model, bad solvent; column B, heterogeneous chain model, bad solvent; column C, hydrostatic driving force, good solvent. Top to bottom: varying degree of translocation: 0, 25, 50, 75, and 100%.

translocation is slow, polymer conformational relaxation is much faster compared to penetration through the pore. The two fragments of the chain located in the *cis* and *trans* compartments behave as tethered subchains. These configurations may be deformed as the driving force becomes stronger and the translocation process faster.[48] β increased with the driving force magnitude well beyond the statistical error. However, Kapahnke et al.[15] actually observed a monotonic decrease of β as the driving force strengthened. Lower $\beta \sim 1$ for stronger driving force was also obtained by Li et al.[28] The detailed analysis of the $\tau-N$ dependence in the process of adsorption driven translocation showed that the linear dependence with $\beta = 1$ holds for strong driving force and gradually deteriorates as the driving force decreases.[60] The dependence on the driving force may also explain the difference between the higher value of β obtained in this work and experimental results obtained for electrostatically driven translocation of single-stranded DNA through membrane nanopores.[4,39] Because of the different opening sizes, channel lengths, and potentials applied, a direct comparison is, unfortunately, problematic.

6. EVOLUTION OF CHAIN CONFORMATION DURING THE TRANSLOCATION PROCESS

Configurations of polymer on the *cis* and *trans* sides have been considered in the literature. Most theoretical studies considered translocating polymer as quasi-static, assuming that chain relaxation is much faster compared to the translocation process itself, as described above. In our simulations, as well as in earlier works reviewed below, the translocations scale is longer but comparable to relaxation scale and these processes cannot be separated. Fyta et al.[61] observed that for $N > 100$ the transverse component of R_g follows a dynamic scaling law of 0.6, close to the Flory exponent of a 3D self-avoiding random walk. Guo et al.[29] found an increase in the mean-square radius of gyration of polymer by the DPD method, which indicates that the polymer elongates in the flow direction during translocation. Feng et al.[25] observed in 3D DPD simulation that, during the translocation process, the size of the *trans* fragment is larger than the size of the *cis* fragment. Luo et al.[62] observed that the *cis* fragment was more stretched than the *trans* fragment due to significant nonequilibrium effects. However, a straightforward comparison with the DPD results is somewhat problematic, since in refs 25 and 62 the polymer beads interacted attractively

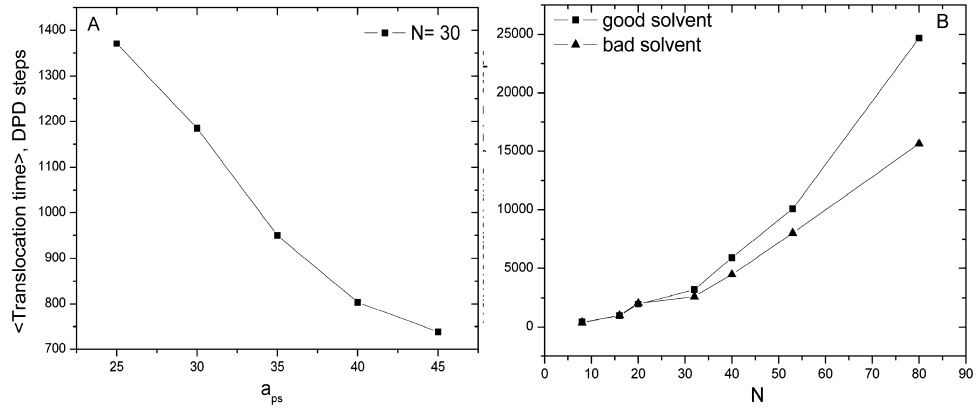

Figure 6. Translocation time dependence on the solvent quality: (a) translocation time dependence on the solvent quality characterized by the solvent–polymer/solvent–solvent interaction contrast, hydrostatic driving force; (b) translocation time dependence of the chain length in good and bad solvents, electrostatic driving force, heterogeneous model.

dx.doi.org/10.1021/jp3104672 | J. Phys. Chem. B 2013, 117, 3648–3658

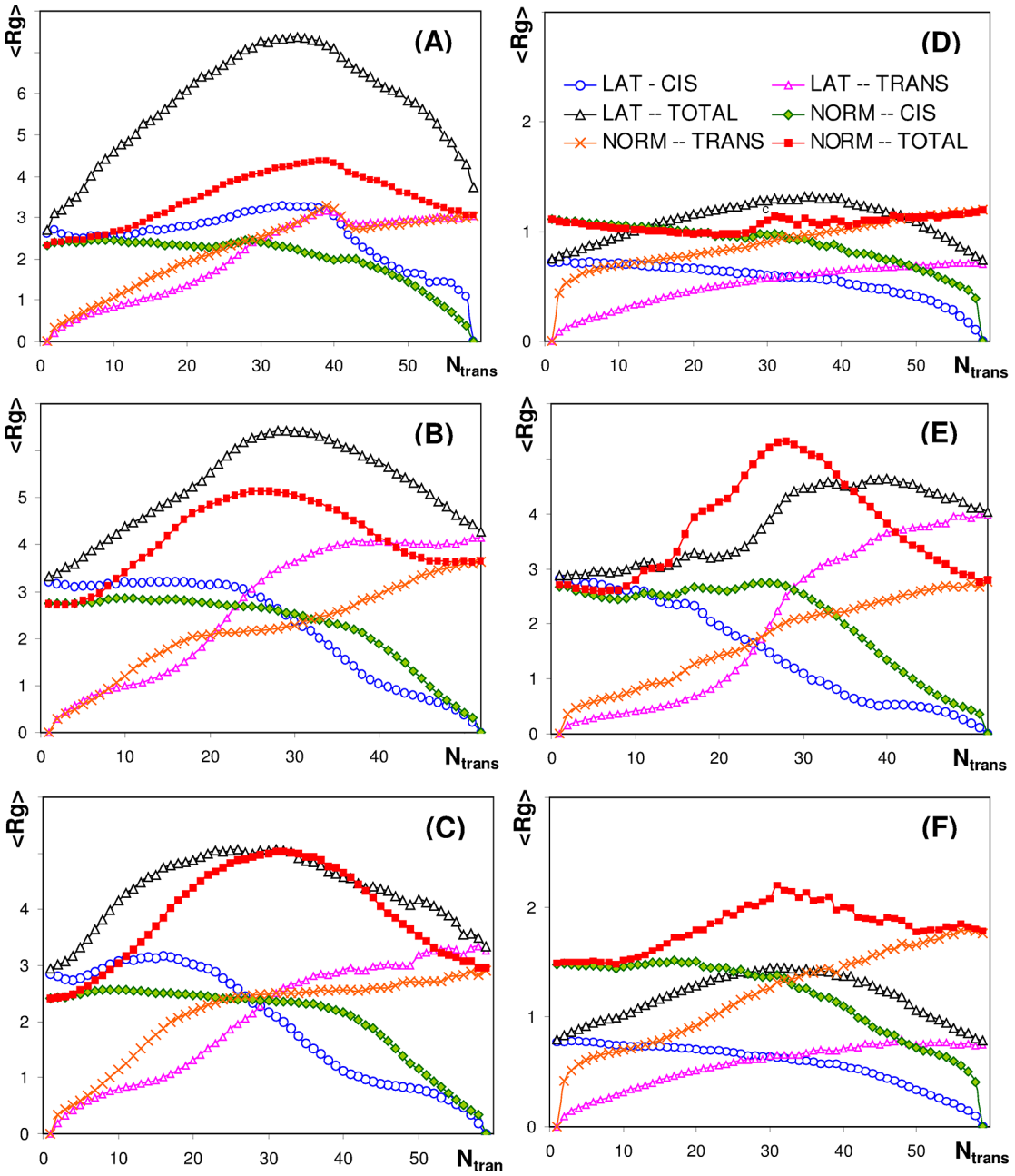

Figure 7. The evolution of lateral (x direction, parallel to the driving field) and normal (yz plane projection, perpendicular to the driving fiels) radii of gyration of the entire chain, *cis* segment, *trans* segment; $N = 60$ for the hydrostatic force and the homogeneous model $N = 53$ for heterogeneous model. Upper panels: uniform hydrostatic force at good (a) and bad (d) solvent conditions. Middle panels: heterogeneous chain model with $E = -1kT/(R_c e)$ (which corresponds to $F = 10\ kT/R_c$ driving force acting on the entire chain) at good (b) and bad (e) solvent conditions. Bottom panels: uniform chain model with the driving force magnitude of $0.1\ kT/R_c$ per bead at good (c) and bad (f) solvent conditions.

via Lennard-Jones interactions between the particles, and the scaling relationships obtained depended on the ratio between the Lennard-Jones particle radius and the radius of dissipative forces. For example, the gyration radius R_g of the *trans* fragment determined in ref 25 fulfilled the scaling relationship $R_g \sim N_{trans}^{0.79}$ for smaller dissipative radius and $R_g \sim N_{trans}^{0.64}$ for larger dissipative radius. Even in the case of unbiased translation, nonequilibrium effects were evident.[63]

To study how the chain conformation changes during the translocation process, we considered conformations of *cis* and *trans* fragments of the translocating chain separately as a function of degree of translocation, here defined as N_{trans}, the number of monomers that has moved to the *trans* side. Figure 7 demonstrates the evolution of the *cis* and *trans* radii of gyration in the normal and lateral direction during the translocation process. The data points presented are averaged over series that include no less than 1000 successful translocations each. The results of events with failed translocation are also included in the average R_g presented in Figure 7. The plots of R_g vs N are more instructive in normal, rather than logarithmic, coordinates. Since the chain length was limited to 60 or 53 beads, the scaling analysis cannot be performed and, indeed, the log–log plots did not contain well-defined linear regions in any reasonable length intervals.

Under good solvent conditions, translocation starts from an asymmetric coil-like *cis* chain (Figure 5b,c). As the *trans*

dx.doi.org/10.1021/jp3104672 | J. Phys. Chem. B 2013, 117, 3648–3658

segment starts growing, the R_g for the *cis* segment changes very little or even shows a slight increase, visible for hydrostatic force (Figure 7a). Hydrostatic force affects polymers and solvents alike, creating a flow of solvent, with the velocities of particles at the narrow opening much faster than in the middle of the *cis* or *trans* compartments. The solvent flow, which is developing as the polymer is pulled through the opening, apparently makes the polymer accept a conformation stretched in the lateral direction. In both compartments, the polymer is expanded compared to a normal coil, as the lateral R_g achieves a maximum far exceeding that of a chain composed of two tethered equilibrium coils. In the final configuration, the polymer is more extended than in the initial configuration.

Strong nonequilibrium effects and asymmetric chain geometry were also observed with the heterogeneous chain model. The initial conformations of the chain are more extended than the normal tethered coil conformations used with the hydrostatic force, apparently due to electrostatic forces between the charged monomers. Radii of gyration monotonically decrease in the *cis* and increase in the *trans* compartment as the polymer proceeds through the opening, showing that nonmonotonic behavior observed under hydrostatic force these effects should be attributed to the solvent flow. Still, the maximum R_g for the heterogeneous model in good solvent exceeds that of a chain composed of two tethered equilibrium coils, and the final conformation of the chain is more extended in the lateral direction than the initial conformation (Figure 7b). Both uneven charge distribution and existence of mobile counterions might have contributed to the nonequilibrium effects. First, the middle segment experiences a force opposite the translocation direction, which causes translocation to slow down. Second, counterions are much more mobile compared to the polymer. Therefore, anions create a cocurrent flow and cations create a counter-flow through the opening. The separation of cations from the polyelectrolyte contributes to the expansion of the latter due to uncompensated electrostatic repulsion between the chain anions. This force vanishes when the cation counterflow is established, and they become distributed more or less homogeneously over the system volume. This may be the reason for slower translocation and nearly constant R_g for the *cis* segment at the initial stage of translocation, seen in Figure 7b.

With the uniform model, where the driving force is applied to polymer beads only, nonequilibrium effects in that system were also evident: the power law correlation $R_g \sim (N-1)^{\nu}$ was completely inapplicable in either compartment. The polymer chain, however, was rather symmetric, with R_g on the *trans* side approximately equal to that on the *cis* side of the same length, in lateral and normal directions alike (Figure 7c).

In bad solvent, the polymer adopted globular configurations at the start of translocation and is threaded through the opening, gradually entering a globule that forms on the other side. This scenario was observed under hydrostatic driving force and with the homogeneous chain model (Figure 7d,f). The configurations of the chain were rather symmetric, with $R_g(N)$ showing similar behavior for the *trans* and *cis* segments. Nevertheless, the scaling relationship $R_g \sim (N-1)^{\nu}$ was inapplicable in *cis* and *trans* compartments alike. Because the heterogeneous chain model in this paper does not exhibit a true coil−globule transition, translocation in bad solvent was rather similar to that in good solvent, as was already demonstrated already by τ vs N scaling (Figure 7e).

7. CONCLUSIONS AND DISCUSSION

We present the first three-dimensional DPD simulation study of the forced translocation, which explicitly takes into account electrostatic interactions between the charged monomers and solution counterions. Translocation of a polymer chain through a membrane nanopore driven by an applied force was extensively studied in the literature using a variety of experimental and theoretical techniques, and there is a substantial disagreement among the published data. We considered the dependence of the translocation time τ on a variety of factors, such as the chain length N, the driving force magnitude E, and the solvent quality characterized by the solvent−polymer interaction parameter a_{PS}, which was varied in the range from 0 to $45kT/R_c$ that should be compared with the solvent−solvent interaction parameter $a_{ss} = 25kT/R_c$. The simulation results were interpreted in terms of scaling exponents β and ξ obtained from linear correlations in double logarithmic coordinates, assuming scaling relationships $\tau \sim N^{\beta}$ and $\tau \sim E^{-\xi}$, respectively. The chain conformation was characterized by the Flory exponent ν calculated from the chain length dependence of the radius of gyration, $R_g \sim N^{\nu}$. The evolution of chain conformations in the process of translocation was explored by monitoring the radii of gyration of the *cis* and *trans* fragments of the translocating chain in normal and lateral directions.

We considered two types of driving force: the uniform hydrostatic-type force acting on both solvent and polymer and the uniform electrostatic-type force acting on the selected or all (charged) chain beads and selected (counter-charged) solvent beads. In the electrostatic case, two types of charge distributions along the chain were assigned: uniform and heterogeneous. In the latter, the charge distribution corresponded to that in βLGa. These models were chosen for their simplicity and qualitative difference; in the uniform chain model, the force is proportional to the chain length, while in the protein model the force is independent of the chain length. A realistic consideration of DNA, which bears a large negative charge, is hardly possible without a large solvent bath with added electrolyte, which would make a reliable collection of statistics performed in this work unfeasible. In the case of a heterogeneous model that roughly describes protein translocation, the very consideration of polyion conformation under different solvent conditions is actually a major challenge, as it has not been analyzed before.

To set a reference, we explored the coil−globule transition in free chains by varying the solvent quality parameter a_{PS}. For the system studied, we found a gradual transition from $\nu = 0.55$ to 0.6 under good solvent conditions ($a_{PS} = 25\ kT/R_c$) to $\nu = 0.3$ under bad solvent conditions ($a_{PS} = 40$) with the θ-point value of $\nu = 0.5$ achieved at $a_{PS} = 27.25\ kT/R_c$. It is worth noting that, for the limited chain length (<100 beads), the θ transition is pretty gradual with the Flory exponent continuously varied from ∼0.6 at $a_{PS} \approx 15$ to ∼0.3 and $a_{PS} \approx 30$ crossing the ideal value of 0.5 at $a_{PS} = 27.25$.

The scaling correlations, $\tau \sim E^{-\xi}$ and $\tau \sim N^{\beta}$, were established only for coil-like chains, and could not be identified with a reasonable accuracy for globular chains. Regardless of the type of the driving force, we found the driving force exponent $\xi \approx 0.9$. This generally confirms the approximate inverse-proportional correlation between the translocation time and driving force magnitude ($\xi = 1$) reported previously in the majority of published experimental and theoretical studies. This

dx.doi.org/10.1021/jp3104672 | J. Phys. Chem. B 2013, 117, 3648−3658

conclusion agrees with published experimental and modeling data.[4,49]

The obtained correlation between the translocation time τ and the chain length N with the scaling exponent $\beta \approx 1.44$ for coils in good solvent driven by the hydrostatic force agrees with the $\beta = 1 + \nu$ relationship between the translocation exponent β and the Flory exponent ν suggested in some of the published theoretical works.[18,21] However, simulations of the systems with different solvent quality showed that the $\beta = 1 + \nu$ relationship did not hold for bad solvent conditions. In contrast, we found that, as the solvent quality worsens, β increases and the accuracy of linear regression analysis deteriorates. That is, the influence of the chain length on the translocation time is stronger in bad solvent compared to good solvent. For the electrostatic driving force, we observed larger values of $\beta \approx 1.7-1.9$ depending on the charge distribution along the chain. One may speculate that this difference was caused by the different mechanisms of chain−solvent interactions: in the hydrostatic case, the chain and solvent coflow, while in the electrostatic case, oppositely charged counterions cause additional chain−solvent friction.

The chain conformations of the translocating chains analyzed from the variation of the gyration radii of *cis* and *trans* fragments showed strong nonequilibrium effects for all systems, especially pronounced under the hydrostatic driving force that creates a solvent flow with very nonuniform particle velocities. In good solvent, the nonequilibrium effects lead to extended and asymmetric conformations of the chain. Translocation of globules occurred faster than translocation of coils of the same length that is somewhat counterintuitive. This effect is related to the definition of the translocation time that we adopted. Indeed, the clock started when the chain end penetrated into the pore, so that the time needed for the chain end to reach the pore is not counted. And once the translocation started, the chain threaded out of the globule experienced less hydrodynamic friction than the chain threaded out of the coil. We did not observe the globule opening up during the translocation process. The chain adopted a symmetric globular configuration on the *cis* and *trans* sides alike.

The methodological novelty of this work is in the demonstration of the feasibility of the 3D DPD method for modeling the translocation phenomena under different conditions and accounting for the electrostatic interactions with explicit counterions, as well as for the solvent quality, in a computationally efficient manner (compared with hard-core potential models). Further studies should involve customization of the coarse-graining procedure to reflect the complex structure of biopolymers of practical interest. This would require introduction of different chain beads, incorporation of side subchains, and multicomponent solvent solutions, including added electrolyte that contributes to screening of the electrostatic interactions between monomers and counterions. Also, the driving force should be considered as spatially distributed; in the electrostatic case, this distribution can be obtained from the simultaneous solution of the Poisson−Boltzmann equation.

■ ASSOCIATED CONTENT

Supporting Information

Charge profile of β-lactoglobulin at normal pH and its mapping on model polymers of different chain lengths used in translocation simulations with the heterogeneous chain model. This material is available free of charge via the Internet at http://pubs.acs.org.

■ AUTHOR INFORMATION

Corresponding Author

*E-mail: aneimark@rci.rutgers.edu.

Notes

The authors declare no competing financial interest.

■ ACKNOWLEDGMENTS

This work was supported in part by the PRF-ACS Grant No. 48890-ND6, NSF CBET Grant No. 1064170, National Basic Research Program (973) of China (No. 2012CB214803), and National Science Foundation of China (Grant No. 41103029).

■ REFERENCES

(1) Alberts, B.; Bray, D. *Molecular Biology of the Cell*; Garland: New York, 1994.
(2) Darnell, J.; Lodish, H.; Baltimore, D. *Molecular Cell Biology*; Scientific American Books: New York, 1995.
(3) Movileanu, L. Interrogating Single Proteins through Nanopores: Challenges and Opportunities. *Trends Biotechnol.* **2009**, *27*, 333−341.
(4) Kasianowicz, J. J.; Brandin, E.; Branton, D.; Deamer, D. W. Characterization of Individual Polynucleotide Molecules Using a Membrane Channel. *Proc. Natl. Acad. Sci. U.S.A.* **1996**, *93*, 13770−13773.
(5) Talaga, D. S.; Li, J. Single-Molecule Protein Unfolding in Solid State Nanopores. *J. Am. Chem. Soc.* **2009**, *131*, 9287−9297.
(6) Schibel, A. E. P.; An, N.; Jin, Q. A.; Fleming, A. M.; Burrows, C. J.; White, H. S. Nanopore Detection of 8-Oxo-7,8-Dihydro-2′-Deoxyguanosine in Immobilized Single-Stranded DNA via Adduct Formation to the DNA Damage Site. *J. Am. Chem. Soc.* **2010**, *132*, 17992−17995.
(7) Chu, J.; Gonzalez-Lopez, M.; Cockroft, S. L.; Amorin, M.; Ghadiri, M. R. Real-Time Monitoring of DNA Polymerase Function and Stepwise Single-Nucleotide DNA Strand Translocation through a Protein Nanopore. *Angew. Chem., Int. Ed.* **2010**, *49*, 10106−10109.
(8) Aksimentiev, A. Deciphering Ionic Current Signatures of DNA Transport through a Nanopore. *Nanoscale* **2010**, *2*, 468−483.
(9) Bhattacharya, S.; Derrington, I. M.; Pavlenok, M.; Niederweis, M.; Gundlach, J. H.; Aksimentiev, A. Molecular Dynamics Study of Mspa Arginine Mutants Predicts Slow DNA Translocations and Ion Current Blockades Indicative of DNA Sequence. *ACS Nano* **2012**, *6*, 6960−6968.
(10) Sung, W.; Park, P. J. Polymer Translocation through a Pore in a Membrane. *Phys. Rev. Lett.* **1996**, *77*, 783−786.
(11) Park, P. J.; Sung, W. Polymer Translocation Induced by Adsorption. *J. Chem. Phys.* **1998**, *108*, 3013−3018.
(12) Muthukumar, M. Polymer Escape through a Nanopore. *J. Chem. Phys.* **2003**, *118*, 5174.
(13) Chern, S. S.; Cárdenas, A. E.; Coalson, R. D. Three-Dimensional Dynamic Monte Carlo Simulations of Driven Polymer Transport through a Hole in a Wall. *J. Chem. Phys.* **2001**, *115*, 7772−7782.
(14) Muthukumar, M.; Kong, C. Y. Simulation of Polymer Translocation through Protein Channels. *Proc. Natl. Acad. Sci. U.S.A.* **2006**, *103*, 5273−5278.
(15) Kapahnke, F.; Schmidt, U.; Heermann, D. W.; Weiss, M. Polymer Translocation through a Nanopore: The Effect of Solvent Conditions. *J. Chem. Phys.* **2010**, *132*, 164904.
(16) Kantor, Y.; Kardar, M. Anomalous Dynamics of Forced Translocation. *Phys. Rev. E* **2004**, *69*, 021806.
(17) Lubensky, D. K.; Nelson, D. R. Driven Polymer Translocation through a Narrow Pore. *Biophys. J.* **1999**, *77*, 1824−1838.
(18) Tsuchiya, S.; Matsuyama, A. Translocation and Insertion of an Amphiphilic Polymer. *Phys. Rev. E* **2007**, *76*, 011801.

(19) Loebl, H. C.; Randel, R.; Goodwin, S. P.; Matthai, C. C. Simulation Studies of Polymer Translocation through a Channel. *Phys. Rev. E* **2003**, *67*, 041913.
(20) Milchev, A.; Binder, K.; Bhattacharya, A. Polymer Translocation through a Nanopore Induced by Adsorption: Monte Carlo Simulation of a Coarse-Grained Model. *J. Chem. Phys.* **2004**, *121*, 6042−6051.
(21) Dubbeldam, J. L. A.; Milchev, A.; Rostiashvili, V. G.; Vilgis, T. A. Driven Polymer Translocation through a Nanopore: A Manifestation of Anomalous Diffusion. *Europhys. Lett.* **2007**, *79*, 18002.
(22) Romiszowski, P.; Sikorski, A. Monte Carlo Study of Polymer Translocation through a Hole. *Comput. Mater. Sci.* **2007**, *38*, 533−537.
(23) Matysiak, S.; Montesi, A.; Pasquali, M.; Kolomeisky, A. B.; Clementi, C. Dynamics of Polymer Translocation through Nanopores: Theory Meets Experiment. *Phys. Rev. Lett.* **2006**, *96*, 118103.
(24) Bernaschi, M.; Melchionna, S.; Succi, S.; Fyta, M.; Kaxiras, E. Quantized Current Blockade and Hydrodynamic Correlations in Biopolymer Translocation through Nanopores: Evidence from Multiscale Simulations. *Nano Lett.* **2008**, *8*, 1115−1119.
(25) Feng, J. A.; Ge, X. T.; Shang, Y. Z.; Zhou, L. H.; Liu, H. L.; Hu, Y. Translocation of Polymer through a Nanopore Studied by Dissipative Particle Dynamics. *Fluid Phase Equilib.* **2011**, *302*, 26−31.
(26) Yong, H. S.; Wang, Y. L.; Yuan, S. C.; Xu, B.; Luo, K. F. Driven Polymer Translocation through a Cylindrical Nanochannel: Interplay between the Channel Length and the Chain Length. *Soft Matter* **2012**, *8*, 2769−2774.
(27) Tian, P.; Smith, G. D. Translocation of a Polymer Chain across a Nanopore: A Brownian Dynamics Simulation Study. *J. Chem. Phys.* **2003**, *119*, 11475−11483.
(28) Li, X. J.; Li, X. L.; Deng, M. G.; Liang, H. J. Effects of Electrostatic Interactions on the Translocation of Polymers through a Narrow Pore under Different Solvent Conditions: A Dissipative Particle Dynamics Simulation Study. *Macromol. Theory Simul.* **2012**, *21*, 120−129.
(29) Guo, J. Y.; Li, X. J.; Liu, Y.; Liang, H. J. Flow-Induced Translocation of Polymers through a Fluidic Channel: A Dissipative Particle Dynamics Simulation Study. *J. Chem. Phys.* **2011**, *134*, 8.
(30) Wei, D.; Yang, W.; Jin, X.; Liao, Q. Unforced Translocation of a Polymer Chain through a Nanopore: The Solvent Effect. *J. Chem. Phys.* **2007**, *126*, 204901.
(31) Forrey, C.; Muthukumar, M. Langevin Dynamics Simulations of Ds-DNA Translocation through Synthetic Nanopores. *J. Chem. Phys.* **2007**, *127*, 015102.
(32) He, Y. D.; Qian, H. J.; Lu, Z. Y.; Li, Z. S. Polymer Translocation through a Nanopore in Mesoscopic Simulations. *Polymer* **2007**, *48*, 3601−3606.
(33) Vishnyakov, A.; Talaga, D. S.; Neimark, A. V. DPD Simulation of Protein Conformations: From Alpha-Helices to Beta-Structures. *J. Phys. Chem. Lett.* **2012**, *3*, 3081−3087.
(34) Hoogerbrugge, P. J.; Koelman, J. M. V. A. Simulating Microscopic Hydrodynamic Phenomena with Dissipative Particle Dynamics. *Europhys. Lett.* **1992**, *19*, 155−160.
(35) Groot, R.; Warren, P. Dissipative Particle Dynamics: Bridging the Gap between Atomistic and Mesoscopic Simulation. *J. Chem. Phys.* **1997**, *107*, 4423−4435.
(36) Groot, R. D. Mesoscopic Simulation of Polymer−Surfactant Aggregation. *Langmuir* **2000**, *16*, 7493−7502.
(37) Groot, R. D. Electrostatic Interactions in Dissipative Particle Dynamics—Simulation of Polyelectrolytes and Anionic Surfactants. *J. Chem. Phys.* **2003**, *118*, 11265−11277.
(38) Wang, Y. L.; Lu, Z. Y.; Laaksonen, A. Specific Binding Structures of Dendrimers on Lipid Bilayer Membranes. *Phys. Chem. Chem. Phys.* **2012**, *14*, 8348−8359.
(39) Meller, A.; Nivon, L.; Branton, D. Voltage-Driven DNA Translocations through a Nanopore. *Phys. Rev. Lett.* **2001**, *86*, 3435−3438.
(40) Ilnytskyi, J. M.; Holovatch, Y. How Does the Scaling for the Polymer Chain in the Dissipative Particle Dynamics Hold? *Condens. Matter Phys.* **2007**, *10*, 539−551.
(41) Spenley, N. A. Scaling Laws for Polymers in Dissipative Particle Dynamics. *Europhys. Lett.* **2000**, *49*, 534−540.
(42) Jiang, W.; Huang, J.; Wang, Y.; Laradji, M. Hydrodynamic Interaction in Polymer Solutions Simulated with Dissipative Particle Dynamics. *J. Chem. Phys.* **2007**, *126*, 044901.
(43) Meller, A.; Branton, D. Single Molecule Measurements of DNA Transport through a Nanopore. *Electrophoresis* **2002**, *23*, 2583−2591.
(44) Storm, A. J.; Storm, C.; Chen, J.; Zandbergen, H.; Joanny, J.-F.; Dekker, C. Fast DNA Translocation through a Solid-State Nanopore. *Nano Lett.* **2005**, *7*, 1193−1197.
(45) Gauthier, M. G.; Slater, G. W. A Monte Carlo Algorithm to Study Polymer Translocation through Nanopores. I. Theory and Numerical Approach. *J. Chem. Phys.* **2008**, *128*, 065103.
(46) Lehtola, V. V.; Linna, R. P.; Kaski, K. Critical Evaluation of the Computational Methods Used in the Forced Polymer Translocation. *Phys. Rev. E* **2008**, *78*, 061803.
(47) Barker, C. E.; Dallegge, T. Secondary Gas Emissions During Coal Desorption, Marathon Grassim Oskolkoff-1 Well, Cook Inlet Basin, Alaska: Implications for Resource Assessment. *Bull. Can. Pet. Geol.* **2006**, *54*, 273−291.
(48) Huopaniemi, I.; Luo, K.; Ala-Nissila, T.; Ying, S.-C. Langevin Dynamics Simulations of Polymer Translocation through Nanopores. *J. Chem. Phys.* **2006**, *125*, 124901.
(49) Ikonen, T.; Bhattacharya, A.; Ala-Nissila, T.; Sung, W. Influence of Non-Universal Effects on Dynamical Scaling in Driven Polymer Translocation. *J. Chem. Phys.* **2012**, *137*, 085101.
(50) Chen, Y.-C.; Wang, C.; Zhou, Y.-L.; Luo, M.-B. Effect of Attractive Polymer-Pore Interactions on Translocation Dynamics. *J. Chem. Phys.* **2009**, *130*, 054902.
(51) Luo, K.; Ala-Nissila, T.; Ying, S.-C.; Bhattacharya, A. Translocation Dynamics with Attractive Nanopore-Polymer Interactions. *Phys. Rev. E* **2008**, *78*, 061918.
(52) Bhattacharya, A.; Morrison, W. H.; Luo, K.; Ala-Nissila, T.; Ying, S.-C.; Milchev, A.; Binder, K. Scaling Exponents of Forced Polymer Translocation through a Nanopore. *Eur. Phys. J. E* **2009**, *29*, 423−429.
(53) Zhu, F. Q.; Tajkhorshid, E.; Schulten, K. Theory and Simulation of Water Permeation in Aquaporin-1. *Biophys. J.* **2004**, *86*, 50−57.
(54) Mamonov, A. B.; Coalson, R. D.; Zeidel, M. L.; Mathai, J. C. Water and Deuterium Oxide Permeability through Aquaporin 1: MD Predictions and Experimental Verification. *J. Gen. Physiol.* **2007**, *130*, 111−116.
(55) Chen, Z.; Jiang, Y.; Dunphy, D. R.; Adams, D. P.; Hodges, C.; Liu, N.; Zhang, N.; Xomeritakis, G.; Jin, X.; Aluru, N. R.; et al. DNA Translocation through an Array of Kinked Nanopores. *Nat. Mater.* **2010**, *9*, 667−675.
(56) Chen, Y. C.; Wang, C.; Luo, M. B. Simulation Study on the Translocation of Polymer Chains through Nanopores. *J. Chem. Phys.* **2007**, *127*, 044904.
(57) Panja, D.; Barkema, G. T.; Ball, R. C. Polymer Translocation out of Planar Confinements. *J. Phys.: Condens. Matter* **2008**, *20*, 075101.
(58) Muthukumar, M. Polymer Translocation through a Hole. *J. Chem. Phys.* **1999**, *111*, 10371−10374.
(59) Qian, H.; Sun, L. Z.; Luo, M. B. Simulation Study on the Translocation of a Partially Charged Polymer through a Nanopore. *J. Chem. Phys.* **2012**, *137*.
(60) Yang, S.; Neimark, A. V. Adsorption-Driven Translocation of Polymer Chain into Nanopores. *J. Chem. Phys.* **2012**, 136.
(61) Fyta, M.; Melchionna, S.; Succi, S.; Kaxiras, E. Hydrodynamic Correlations in the Translocation of a Biopolymer through a Nanopore: Theory and Multiscale Simulations. *Phys. Rev. E* **2008**, *78*, 036704.
(62) Luo, K.; Huopaniemi, I.; Ala-Nissila, T.; Ying, S.-C. Polymer Translocation through a Nanopore under an Applied External Field. *J. Chem. Phys.* **2006**, *124*, 114704.
(63) Gauthier, M. G.; Slater, G. W. Nondriven Polymer Translocation through a Nanopore: Computational Evidence That the Escape and Relaxation Processes Are Coupled. *Phys. Rev. E* **2009**, *79*, 021802.